EPJ manuscript No.
(will be inserted by the editor)

Pion-nucleon charge-exchange amplitudes above 2 GeV

F. Huang[1], A. Sibirtsev[2], S. Krewald[1], C. Hanhart[1], J. Haidenbauer[1], and U.-G. Meißner[1,2]

[1] Institut für Kernphysik and Jülich Center for Hadron Physics, Forschungszentrum Jülich, D-52425 Jülich, Germany
[2] Helmholtz-Institut für Strahlen- und Kernphysik (Theorie) and Bethe Center for Theoretical Physics, Universität Bonn, Nußallee 14-16, D-53115 Bonn, Germany

Received: date / Revised version: date

Abstract. The amplitudes for the pion-nucleon charge exchange reaction of the Karlsruhe-Helsinki and the George-Washington-University partial wave analyses are compared with those of a Regge-cut model with the aim to explore the possibility to provide high energy constraints for theoretical baryon resonance analyses in the energy region above 2 GeV.

PACS. 13.75.-n Hadron-induced low- and intermediate energy reactions – 14.20.Gk Baryon resonances with S=0 – 11.55.Jy Regge formalism

1 Introduction

Presently there is intense experimental activity to study baryon resonances in the energy range up to 2.4 GeV [1,2,3,4]. Nearly all established resonances summarized in the Review of Particle Physics [5] were obtained in the time period before 1980 from partial wave analyses of pion-nucleon reactions by the Karlsruhe-Helsinki (KH80) [6,7] and the Carnegie-Mellon-Berkeley (CMB) [8] collaborations. Arndt and his collaborators at the George Washington University (GWU) have published a series of more recent analyses [9,10] including the enlarged data basis provided by LAMPF, TRIUMF, and PSI which cast doubt on some of the resonances found in previous analyses. New data on spin rotation parameters obtained by the ITEP-PNPI collaborations showed some limitations of the KH80 and the CMB analyses [12,13,14].

The experimental data on $\pi\pi N$, ηN, and $K\Lambda$ final states require unitary multichannel resonance parameterizations [15,16,17,18]. The physical background due to non-resonant processes employed in those calculations may show a non-trivial energy dependence which is reflected in the extracted resonance parameters and calls for further theoretical developments [18]. The K-matrix approach to coupled-channel reactions combines resonances and non-resonant processes, using effective Lagrangians. Resonance parameters were extracted using the K-matrix method in the energy range up to $\sqrt{s} = 2$ GeV [19]. The K-matrix approach relies on one major approximation, the omission of the real part of the intermediate meson-nucleon propagator. This may affect the details of the non-resonant background. Moreover, it impedes the possibility to generate poles in the S-matrix dynamically – a feature which is strongly emphasized in recent works that apply concepts from effective field theories to meson-meson and meson-baryon scattering [20,21,22,23]. Several groups have developped models for meson-nucleon dynamics based on effective Lagrangians going beyond the K-matrix approximation and studied pion-nucleon scattering for energies up to around 2 GeV [24,25,26,27,28].

An extension of meson-nucleon coupled channel approaches to energies above 2 GeV is a rather challenging task. In principle, partial wave amplitudes would provide the most helpful tool for such an extension. There are limitations at large energies, however. In the energy range from 2 GeV to 3.5 GeV, the number of partial waves employed in the KH80 analysis rises, as partial waves up to angular momentum $j = 37/2$ are necessary. Naturally, it is difficult to determine such a large number of parameters from the available data. For very high energies the angular distributions of two-body reactions show well-known regularities: the differential cross sections are dominated by forward scattering. Here an economic description of the t-dependence of the cross sections in forward direction as well as of their energy dependence is given by Regge phenomenology [29], using Regge trajectories as basic degrees of freedom. Therefore, the question arises in how far the amplitudes deduced from such approaches can serve as a guideline for the envisaged extension to higher energies.

In the present paper we survey the available information on the πN scattering amplitudes from 2 GeV up to energies where the reaction can be quantitatively described within Regge phenomenology. Specifically, we consider the amplitudes that result from the partial wave analyses of the GWU group (which reaches up to 2.5 GeV) and the KH80 solution (which covers energies up to 3.49 GeV) and predictions of Regge models, fitted to high energy πN data. We concentrate on the charge exchange pion-nucleon reaction in this work because of the following reason: For Regge pole trajectories, there is a natu-

ral ordering according to the intercept $\alpha(t=0)$ of the trajectory [30]. The pion-nucleon charge exchange reaction $\pi^- p \to \pi^0 n$ is dominated by the ρ-trajectory because the selectivity of the reaction supresses contributions of the Pomeron which is leading for the elastic pion-nucleon scattering. In view of this we consider a simple Regge-cut model which consists of a rho-pole trajectory and a rho-Pomeron cut only and use vertex functions parameterized by a single exponential. In addition, we compare with the results of a more sophisticated Regge parameterization taken from the literature [31].

We consider the present work as a preparatory step for extending coupled-channel approaches of the πN interaction to energies above 2 GeV. Indeed meson-nucleon coupled channel models and Regge models can be considered as two effective theories made for different energy scales which employ the degrees of freedom most economical for the energy range considered. In the case of meson-meson scattering, Regge constraints have been fruitfully used in the classical and recent Roy equation studies, see e.g. [32, 33,34,35,36]. It will be interesting to see whether the same can be achieved also in the context of coupled-channel approaches and the πN system.

The paper is organized as follows. In section 2, we summarize the parameterization of the employed Regge-cut model. The angular distributions and polarizations obtained are shown in section 3 for some selected energies, followed by a discussion of the energy and momentum dependence of the differential cross sections. The resulting amplitudes are presented and discussed in section 4. Conclusions are drawn in section 5.

2 Formalism

The helicity spin non-flip amplitude $\mathcal{M}_\rho^{++}$ and spin-flip amplitude $\mathcal{M}_\rho^{+-}$ due to the ρ-pole exchange contribution to the $\pi^- p \to \pi^0 n$ reaction are parametrized as

$$\mathcal{M}_\rho^{++} = \beta_\rho^{++}\, G_\rho(s,t) \frac{\pi}{\Gamma[\alpha_\rho(t)]}, \tag{1}$$

$$\mathcal{M}_\rho^{+-} = \sqrt{-t}\; \beta_\rho^{+-}\, G_\rho(s,t) \frac{\pi}{\Gamma[\alpha_\rho(t)]}, \tag{2}$$

where β_ρ is the residue function specified later. The Regge propagator is given by

$$G_\rho(s,t) = \frac{1+\xi_\rho \exp\left[-i\pi\alpha_\rho(t)\right]}{\sin[\pi\alpha_\rho(t)]} \left(\frac{q^2}{q_0^2}\right)^{\alpha_\rho(t)}, \tag{3}$$

with $\xi_\rho = -1$ being the signature of the ρ-trajectory. The ρ trajectory $\alpha_\rho(t)$ is taken as

$$\alpha_\rho(t) = 1 - \alpha'_\rho m_\rho^2 + \alpha'_\rho t. \tag{4}$$

The slope parameter α'_ρ is determined by a fit to the data. Furthermore, q in Eq. (3) is the pion momentum in the center-of-mass system and $q_0 = 1$ GeV/c serves as a scale. The factor $\frac{\pi}{\Gamma}$ cancels the poles of the Regge propagator (3) in the scattering region.

The helicity spin non-flip amplitude $\mathcal{M}_c^{++}$ and spin-flip amplitude $\mathcal{M}_c^{+-}$ due to the ρ-cut exchange, which represents the initial and final state interactions, are parametrized as

$$\mathcal{M}_c^{++} = \beta_c^{++}\, G_c(t,s) \frac{\pi}{\Gamma[\alpha_c(t)]} \ln^{-1}(s/s_0), \tag{5}$$

$$\mathcal{M}_c^{+-} = \sqrt{-t}\; \beta_c^{+-}\, G_c(t,s) \frac{\pi}{\Gamma[\alpha_c(t)]} \ln^{-1}(s/s_0), \tag{6}$$

where the prescription of $G_c(t,s)$ is similar to that of $G_\rho(t,s)$ except that $\alpha_\rho(t)$ is replaced by $\alpha_c(t)$. Here $\alpha_c(t)$ is the ρ-cut trajectory taken as

$$\alpha_c(t) = 1 - \alpha'_\rho m_\rho^2 + \frac{\alpha'_\rho \alpha'_P}{\alpha'_\rho + \alpha'_P} t, \tag{7}$$

with $\alpha'_P = 0.1$ GeV^{-2} being the slope of the Pomeron trajectory, which is well defined from the analysis of elastic scattering data. A scale $s_0 = 1$ GeV has been chosen.

The residue functions for all amplitudes are parameterized in a similar way

$$\beta(t) = \beta_0 \exp(bt), \tag{8}$$

where the coupling constant β_0 and the slope b in the exponential formfactor are determined by a fit to the data.

The total helicity spin non-flip amplitude $\mathcal{M}^{++}$ and spin-flip amplitude $\mathcal{M}^{+-}$ are given by the sum of the above amplitudes, i.e.

$$\mathcal{M}^{++} = \mathcal{M}_\rho^{++} + \mathcal{M}_c^{++}, \tag{9}$$

$$\mathcal{M}^{+-} = \mathcal{M}_\rho^{+-} + \mathcal{M}_c^{+-}. \tag{10}$$

The differential cross section is given by

$$\frac{d\sigma}{dt} = \frac{|\mathcal{M}^{++}|^2 + |\mathcal{M}^{+-}|^2}{s\, q^2}\ , \tag{11}$$

and the polarization by

$$P = \frac{2\,\mathrm{Im}\big[\mathcal{M}^{++}\mathcal{M}^{+-*}\big]}{|\mathcal{M}^{++}|^2 + |\mathcal{M}^{+-}|^2}\ . \tag{12}$$

The difference of the $\pi^- p$ and $\pi^+ p$ total cross sections is

$$\Delta\sigma \equiv \sigma_{\pi^- p} - \sigma_{\pi^+ p} = -\frac{4\sqrt{2\pi}}{q\sqrt{s}} \mathrm{Im}\mathcal{M}^{++}(t=0). \tag{13}$$

The parameters are listed in Table 1. Those parameters have been determined by fitting the data on $\pi^- p \to \pi^0 n$ differential cross sections and polarization for pion beam momenta above 4 GeV/c ($\sqrt{s} \geq 3$ GeV) and for four-momentum transfer squared $|t| \leq 2$ GeV^2 [37].

Table 1. Parameters of the ρ-pole and ρ-cut amplitudes.

Parameter	ρ	ρ-cut
β_0^{++}	-23.8±0.3	0.5±0.3
b^{++}	2.5±0.2	0.6±0.4
β_0^{+-}	151.3±1.1	-113.7±2.2
b^{+-}	1.7±0.1	4.3±0.3
α'_ρ=0.81±0.01		

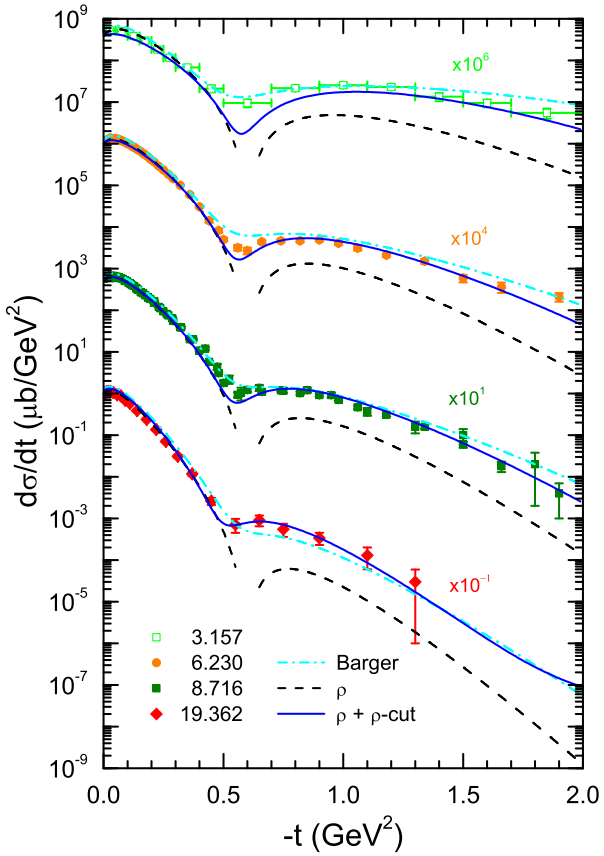

Fig. 1. Differential cross sections for the reaction $\pi^- p \to \pi^0 n$ as a function of the four-momentum transfer squared for different collision energies indicated in the legend. The solid lines represent the results of our Regge-cut model, those based on a pure rho-pole fit are given by the dashed line. Results for the model of Ref. [31] are shown as dash-dotted lines. The data are taken from Refs. [39,40,41,42,43,44,45].

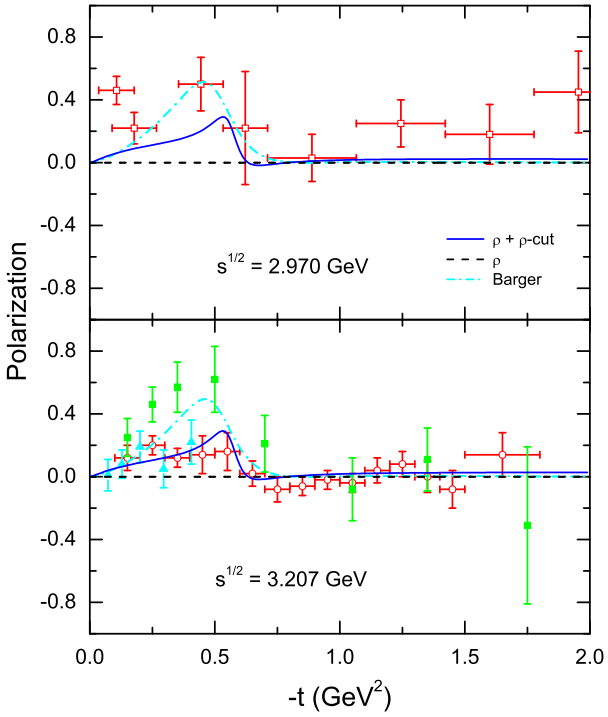

Fig. 2. The polarization in the reaction $\pi^- p \to \pi^0 n$ as a function of four-momentum transfer squared for different collision energies indicated in the legends. Same description of curves as in Fig. 1. The data are taken from Refs. [46] (open squares), [47] (circles), [48] (triangles), and [49] (filled squares).

3 Cross sections and polarization

There are three well-known predictions for the pion-nucleon charge exchange reaction based on the existence of the rho-trajectory: the energy dependence of the total cross section, the existence of a diffractive minimum in the differential cross section in the vicinity of $t = -0.6$ GeV^2, and the relative phase of the real and imaginary parts of the Regge amplitudes which is fixed by the signature factor $\xi(t) = (1+\xi_\rho \exp[-i\pi\alpha_\rho(t)])$ (Eq. (3)) [38]. The Regge limit is supposed to be valid for energies much larger than the momentum transfers, so that for a given energy, the Regge parameterization is expected to deteriorate with increasing magnitude of the momentum transfer. Regge phenomenology modifies the t-dependence of the amplitudes determined from the Regge trajectory by purely phenomenological vertex functions, which allows to optimize the fit to observables. For our Regge-cut model we have chosen a rather simple form of the vertex function, namely an exponential formfactor, cf. Eq. (8). But in the past, Regge phenomenology has used unconventional parameterizations of the vertex functions in order to obtain an even faster decrease of the helicity non-flip amplitude than the one produced by the rho-pole trajectory. Specifically, functions with a zero crossing at $-t \approx 0.2$ GeV^2 were employed in order to account for the crossover phenomenon. (We will come back to this issue in the next section when we discuss the amplitudes.) One of the models where this has been done is the parameterization of Barger and Phillips [31] and, therefore, we will display their results here for comparison.

The differential cross sections and polarizations obtained are shown in Figs. 1 and 2 for a few selected energies. A more systematic comparison with data will be presented elsewhere [37]. Both our Regge-cut model and and the fit of Ref. [31] reproduce the data reasonably well. The major difference between the two fits occurs in the vicinity of the minima close to $-t = 0.6$ GeV^2: the Barger-Phillips fit overestimates the data near the minimum, while the Regge-cut model tends to lie below the data here. In the Regge-cut model, the contribution of the rho-pole dominates both the helicity non-flip and the helicity flip amplitudes. The rho cut amplitudes are a correction which are mainly required to fill the dip near $-t = 0.6$ GeV^2. One observes a maximum of the angular distribution near $-t = 0.03$ GeV^2 which allows to disentangle the helicity flip and non-flip amplitudes, assuming the validity of the Regge approach.

For illustration purposes we consider here also results based on the Regge-pole contribution alone. The dashed lines in Fig. 1 have been obtained using $\beta_0^{++} = -24.62$, $\beta_0^{+-} = 143.29$, $b^{++} = b^{+-} = 2.33$, and α_ρ=0.832. The strength parameters of the flip and non-flip amplitudes for the pure Regge-pole fit differ by about ten percent from the ones shown in Table 1. The angular distributions for small values of $-t$ are well reproduced by the pure Regge-pole model. But the description deteriorates rapidly from about $-t = 0.4$ GeV^2 onwards because the pole trajectory enforces a vanishing amplitude at $-t = 0.6$ GeV^2. Still, the pure Regge-pole model produces a second maximum of the angular distribution, though it underestimates the magnitude of the corresponding cross section significantly.

The maximum of the polarization which occurs close to $-t = 0.5$ GeV^2, c.f. Fig. 2, is correlated with the first minimum of the angular distributions, as expected from Eq. (12). Our Regge-cut model predicts a smaller polarization than the Barger-Phillips parameterization, but the large experimental uncertainties reflected in the various data sets do not allow to discriminate between the fits. As is well-known, the pure Regge-pole model predicts zero polarization.

Fig. 3 shows the total cross section for the reaction $\pi^- p \to \pi^0 n$ as a function of the energy. Here we also include results based on two πN phase shift analyses, namely the ones by the GWU [10] and the Karlsruhe-Helsinki [7] groups. The results for the GWU analysis are those of their current solution taken from the SAID Program [11]. With regard to Karlsruhe-Helsinki we use the preliminary updated solution KH80 as tabulated in Table 2.2.2.2 of Ref. [7]. Though the KH80 solution (and the later KA84 analysis) is, in principle, available from SAID we used the values from the table because *only there* partial waves amplitudes up to very high angular momenta are listed. The SAID Program provides amplitudes only up to orbital angular momenta of $l = 8$. The KH80 analysis employs partial waves with angular momenta up to $l = 11$ around 2.5 GeV and up to $l = 18$ at the highest energy of 3.487 GeV [7]. We found the contributions from those high angular momenta to be essential for obtaining converged results for the observables and, in particular, for reproducing observables as published by Höhler [7]. Note that the GWU analysis SP06 which covers energies up to 2.5 GeV [10] uses partial waves up to $l = 8$.

The Regge-cut model (solid line) is able to reproduce the experimental data down to approximately 3 GeV (lower panel of Fig. 3). Below 3 GeV (upper panel), the extrapolation of the Regge-cut model underestimates the cross section, which suggests the necessity to incorporate resonances. The energy dependence of the total cross sections can be also reproduced by using only the Regge-pole contribution (dashed line).

As far as the partial wave analyses are concerned one can see that the GWU analysis (short dashed line) starts to deviate from the data from around 2.3 GeV onwards, and produces a strongly rising cross section not in agreement with the data. This is expected in view of the deteriorating χ^2 reported in [10]. The Jülich coupled channel

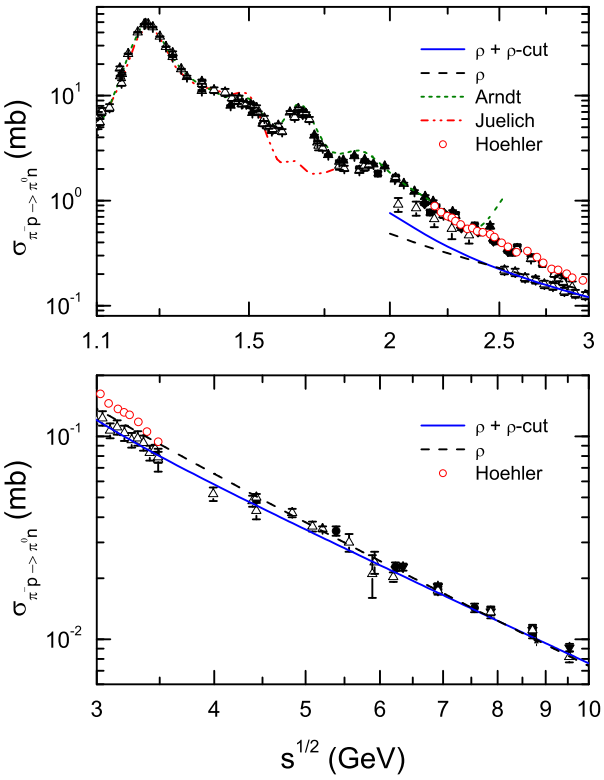

Fig. 3. The $\pi^- p \to \pi^0 n$ total cross sections as a function of the collision energy $\sqrt{s}$. The solid and dashed lines are the results of our Regge-cut model and the pure Regge-pole model, respectively. The short-dashed line represents the results of the partial wave analysis from the GWU group [10] while the open circles are those for the KH80 solution [7]. The dash-dotted line indicates the predictions from the Jülich meson-exchange model [25]. The data are taken from Refs. [39,41,42,49,50,51,52].

meson-exchange model [25] includes only a few low-mass resonances and, consequently, does not agree with the total charge exchange cross sections above 1.5 GeV, cf. the dash-dotted line.

Note that there is a conflict between different data sets in the transition region $2.5 \leq \sqrt{s} \leq 3$ GeV. The Regge fits tend to reproduce the smaller values which seem to be more in line with the high-energy data whereas Höhler's analysis agrees with the larger cross section values in the energy range in question. Those values are compatible with the data at lower energies.

A systematic view of the energy dependence of the differential cross sections for several fixed four-momentum transfers t is provided in Fig. 4. Below $\sqrt{s} \approx 2.5$ GeV, the differential cross sections show bumps which correspond to known resonances, whereas for higher energies the differential cross sections decrease smoothly with energy. The Regge fits are shown down to 3 GeV. In the energy range considered, the Regge cuts are an important contribution to the cross section. For small t the KH80 partial wave analysis joins the results of the two Regge models. With increasing t there is a widening gap between the two Regge

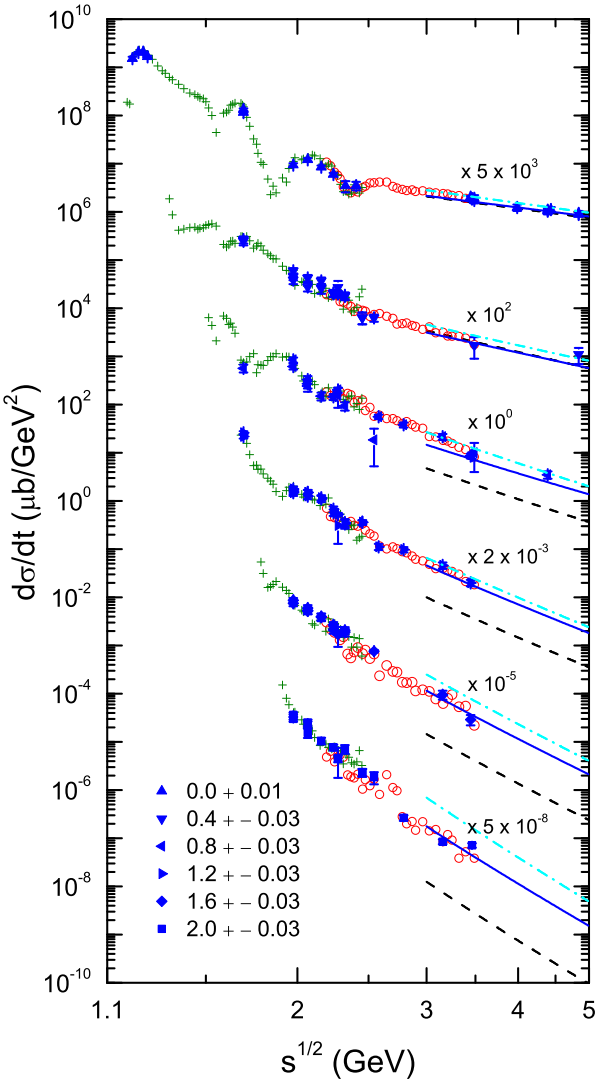

Fig. 4. Differential cross sections for the reaction $\pi^- p \to \pi^0 n$ at fixed t as a function of the collision energy. The $-t$ values considered are 0.0, 0.4, 0.8, 1.2, 1.6, and 2.0 GeV^2 from top to bottom. Same description of curves as in Fig. 1. The "+" symbols represents the results of the partial wave analysis from the GWU group [10] while the open circles are those for the KH80 solution [7]. The data selected for the various intervals of four-momentum transfers squared, as denoted in the legend, are taken from Refs. [39,40,41,42,43,44,45,53,54,55,56].

models, reflecting the different quality of the fits to the data at larger $-t$ values. Obviously, the Barger-Phillips fit overestimates both the available data and the KH80 analysis for $-t \approx 1.6 - 2$ GeV^2. On the other hand, our Regge-cut results are in agreement with the experimental information.

The helicity flip and non-flip cross sections are observables which in principle could be measured directly. The differential cross section for $t = 0$ GeV^2 is entirely determined by the helicity non-flip transition, which opens the possibility to separate the two contributions to the cross section within the Regge model by studying the t-

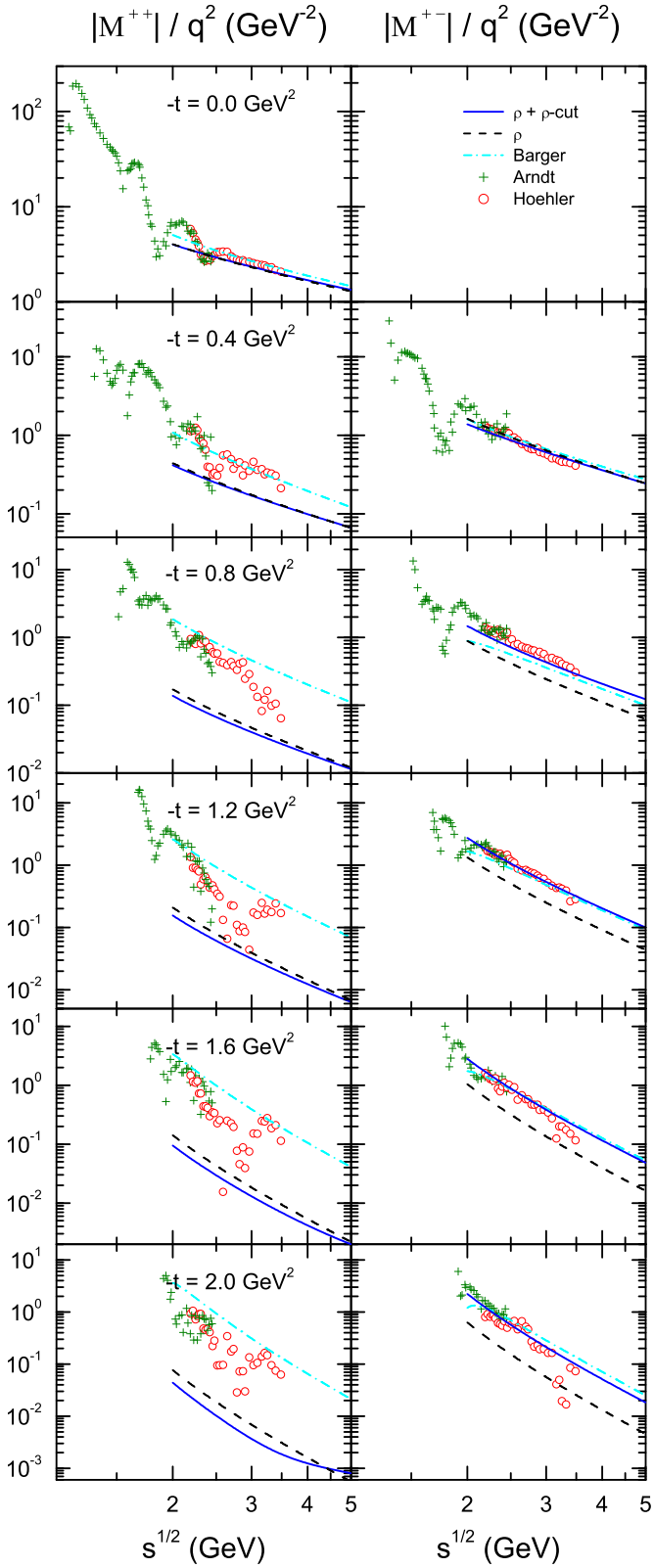

Fig. 5. Moduli of the spin non-flip and spin-flip amplitudes for the reaction $\pi^- p \to \pi^0 n$ divided by the center-of-mass momentum squared at fixed t as a function of the collision energy $\sqrt{s}$. Same description of curves as in Fig. 1. The "+" symbols and the open circles denote the results of the partial wave analyses from the GWU group [10] and the Karlsruhe-Helsinki group (KH80) [7], respectively.

dependence of the cross sections. In Fig. 5, we show the energy dependence of the moduli of the helicity flip and non-flip amplitudes. The moduli of the helicity flip amplitudes predicted by the fit of Ref. [31] (dash-dotted line) and of our Regge-cut model (solid line) are close to each other. The small remaining gap may be taken as a measure for the uncertainty of the determination of the amplitude. The pure Regge-pole fit produces the correct energy dependence, but is unable to provide the magnitude required by the data for $-t$ larger than 0.4 GeV^2, see the dashed line. The KH80 analysis joins the Regge fits smoothly, except for some fluctuations at the largest $|t|$ value considered.

For the helicity non-flip amplitude, the moduli match at $t = 0$ GeV^2, as expected, but at larger four-momentum transfers, considerable differences occur. The Barger-Phillips fit agrees roughly with the KH80 analysis for $\sqrt{s} \geq 2.5$ GeV up to $-t \approx 0.8$ GeV^2, whereas the Regge-cut model produces an amplitude which is much smaller than the KH80 result. The helicity non-flip amplitudes of the KH80 analysis show large fluctuations above 2.5 GeV for all values $-t \geq 0.8$ GeV^2. One should note that the helicity non-flip amplitude is fairly small above $\sqrt{s} \approx 2.5$ GeV, which makes its determination difficult. Direct measurements of polarization and spin rotation parameters for forward angles would help. Recent ITEP experiments have studied other kinematical regimes [13]. Pion beams will be also available at J-PARC. The HADES collaboration at FAIR/GSI [57] prepares a secondary pion beam, which would have to be supplemented by polarized targets.

The total cross-section difference for $\pi^- p$ and $\pi^+ p$ scattering is proportional to the imaginary part of the spin non-flip amplitude for vanishing momentum transfer (see Eq.(13)) and hence can serve as a test whether the amplitude obtained is acceptable. In Fig. 6, we show the difference of the cross sections, multiplied by q^2 to facilitate a comparison on a linear scale. The Regge-cut model (solid line) reproduces the experimental data in the energy interval ranging from 3 GeV to 24 GeV and appears to average the Arndt and Höhler analyses below 3 GeV. The partial wave analyses reflect the presence of resonances, of course. The fact that the Regge amplitude represents quasi an average of the physical amplitude over the resonance region is a manifestation of *duality* in strong interaction physics, a notion extensively discussed and explored in the 1970s (see, e.g., Ref. [64] for a review), and recently revived in the context of interrelating quark- and hadronic degrees of freedom [65].

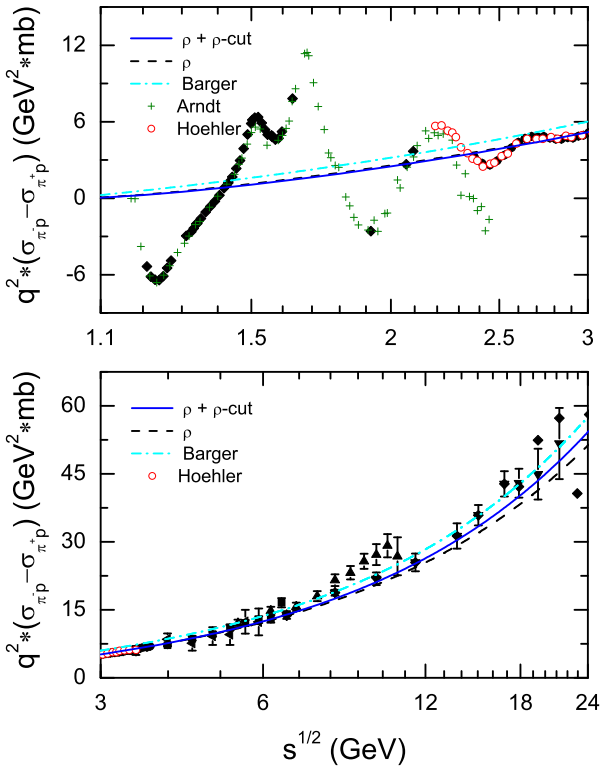

Fig. 6. Total cross-section difference for $\pi^- p$ and $\pi^+ p$ scattering multiplied by the three momentum transfer squared as a function of the collision energy $\sqrt{s}$. Same description of curves as in Fig. 1. The "+" symbols and open circles denote the results of the partial wave analyses from the GWU group [10] and the Karlsruhe-Helsinki group (KH80) [7], respectively. Data are taken from Refs. [5,58,59,60,61,62,63].

4 Amplitudes

After the measurement of spin rotation parameters for $\pi^+ p$ and $\pi^- p$ scattering at a beam momentum of 6 GeV/c, corresponding to $\sqrt{s} = 3.49$ GeV, several πN amplitude analyses were performed at this particular energy [66,67,68]. Since data on $\pi^+ p$ and $\pi^- p$ scattering are much more abundant (see, e.g., [10]) and, in general, also more accurate than for the charge-exchange channel the amplitudes of the partial wave analyses are mainly determined by the former two reactions. On the other hand, in the Regge-model fits considered here only πN charge-exchange data at higher energies have been used as input. It is therefore interesting to compare systematically the amplitudes derived by different methods.

In Fig. 7, we contrast the amplitudes obtained from the present model for the momentum $p_{\rm lab} = 6$ GeV/c with three different amplitude analyses [66,67,68] and the amplitudes generated from the KH80 analysis. The Regge-cute model and the pure rho-pole model produce very similar amplitudes. Both real and imaginary parts of the helicity flip amplitudes are in reasonable agreement with the amplitude analyses. Note, however, that empirically the height of the maximum of the helicity flip amplitude near $-t = 0.2$ GeV^2 is not uniquely determined. The magnitude of the helicity non-flip amplitude for vanishing momentum transfer is fixed by the total cross section data. But the slope of the helicity non-flip amplitude near $t = 0$ differs from the one obtained in the Regge-cut model. Specifically, the zero that appears in Im M^{++} at $t \approx -0.2$ GeV^2, which is commonly connected to the so-called crossover zero in the $\pi^\pm p \to \pi^\pm p$ differential cross sections [30,69,70], is not reproduced by the pure Regge-pole fit but also not by our Regge-cut model. On the other

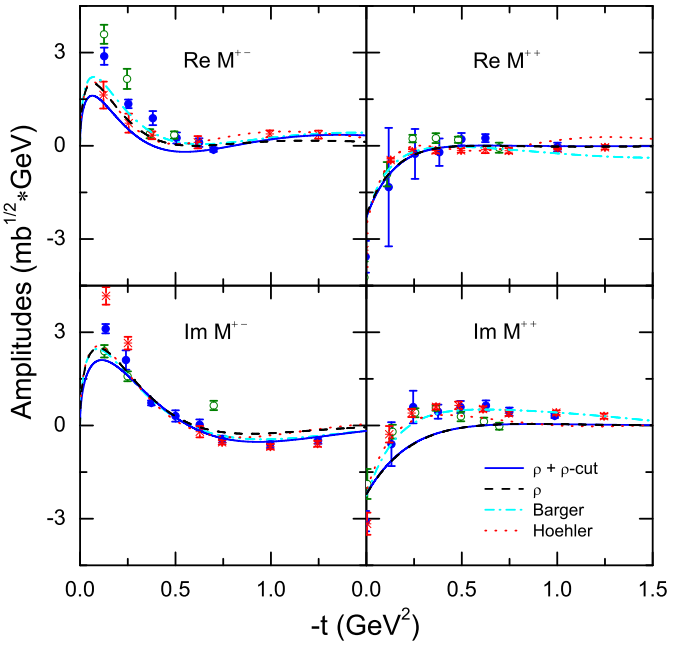

Fig. 7. Spin-flip and spin non-flip amplitudes for the reaction $\pi^- p \to \pi^0 n$ reaction at the collision energy $\sqrt{s} = 3.487$ GeV as a function of the four-momentum transfer squared. Same description of curves as in Fig. 1. The dotted lines are the results of the KH80 analysis [7]. The symbols represent results from different amplitude analyses [66,67,68].

hand, the result based on the Höhler analysis (dotted line) clearly exhibits this feature and is also in good overall agreement with those amplitude analyses.

There have been various suggestions to modify the Regge phenomenology in order to accomodate a vanishing imaginary helicity non-flip amplitude for $-t \approx 0.2$ GeV^2 [30]. In Ref. [31], the vertex function has been modified to generate a zero at $-t \approx 0.2$ GeV^2 in addition to the one produced by the rho-pole trajectory. The t-dependence of the vertex functions assumed in Ref. [31] is entirely phenomenological and might not be optimal for other energies. A comparison with our Regge-cut model which assumes exponentials as vertex functions may therefore be helpful in estimating the systematic uncertainties in Regge models for the helicity non-flip amplitude. One can see in Fig. 7 that the Regge fit by Barger and Phillips describes the zero in Im M^{++} at small $-t$ (dash-dotted line). Note that we have changed the signs of their predictions for Im M^{+-} and Re M^{++} (here and also below) in order to make them comparable to the other results. It remains unclear to us whether this is a matter of conventions only or whether the Barger-Phillips parameterization [31] produced indeed different signs for those amplitudes.

A systematic comparison of the energy dependence of the amplitudes is presented in Figs. 8 and 9. Let us first discuss the real and imaginary parts of the helicity flip amplitudes which are shown in Fig. 8. For energies from around $\sqrt{s} \approx 2.3$ GeV onwards the GWU analysis and the KH80 analysis start to deviate from each other. Our

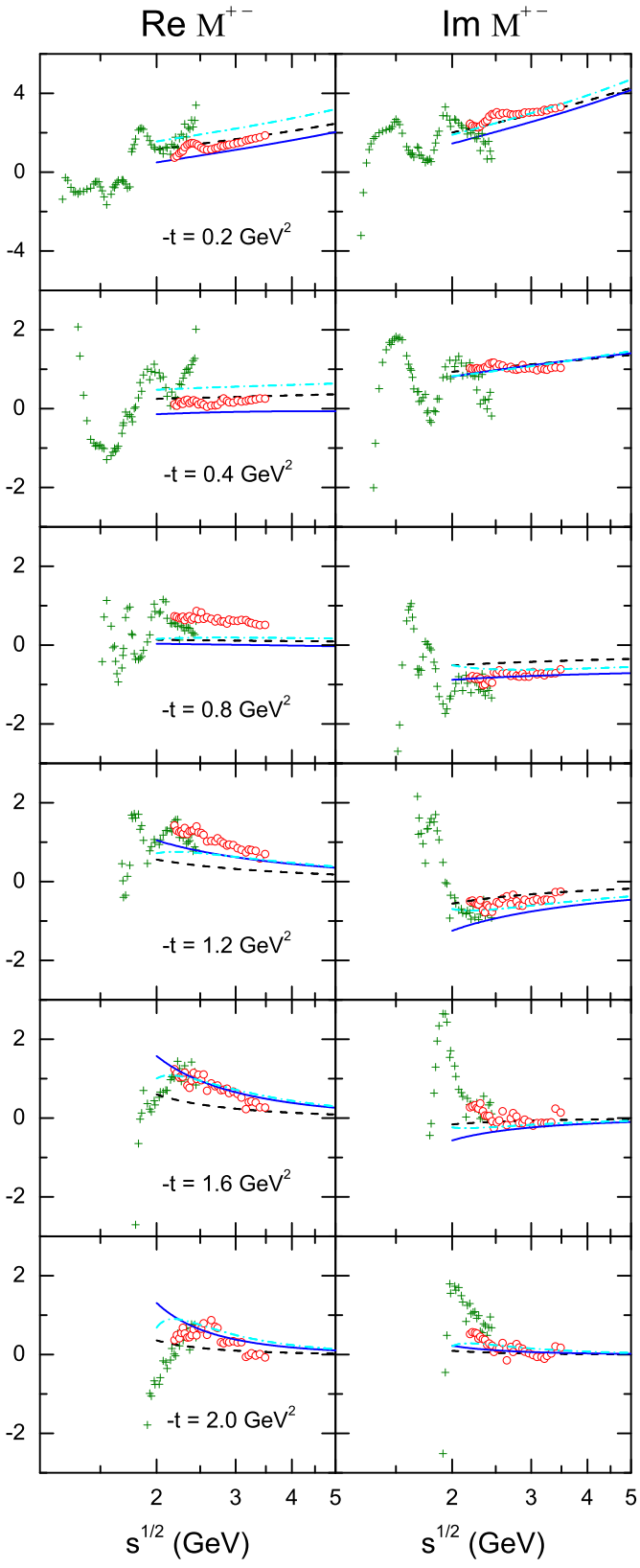

Fig. 8. Helicity flip amplitudes for the reaction $\pi^- p \to \pi^0 n$ at fixed t as a function of the collision energy $\sqrt{s}$. Same description of curves as in Fig. 1. The "+" symbols and the open circles denote the results of the partial wave analyses from the GWU group [10] and the Karlsruhe-Helsinki group (KH80) [7], respectively.

Regge-cut model and the Barger-Phillips parameterization use quite different phenomenological assumptions, yet they produce very similar imaginary parts for the helicity flip amplitude for energies above $\sqrt{s} \approx 3$ GeV. Also the KH80 result is close to the Regge models in this energy region for practically all t-values considered. The real parts of the amplitudes generated by those two Regge fits agree for momentum transfer $-t \geq 0.8$ GeV^2, but show noticeable differences for small $|t|$-values. Moreover, in the latter region neither of them is in line with the KH80 result. The largest differences in the real part of the helicity flip amplitude between the KH80 analysis and the Regge models occurs around $-t \approx 0.8$ GeV^2. Interestingly, the pure Regge-pol fit produces a helicity flip amplitude quite close to the one of the KH80 analysis for $-t \leq 0.4$ GeV^2 (for the real as well as imaginary part), cf. the dashed line in Fig. 8.

The amplitudes for the helicity non-flip amplitudes are shown in Fig. 9. Also here one observes a deviation of the GWU amplitudes from the KH80 result from around 2.3 GeV onwards. For $t = 0$ GeV^2, the KH80 analysis and the two Regge models are in reasonable agreement for energies above $\sqrt{s} \approx 2.5$ GeV. Note that $\mathrm{Im}\, M^{++}(t = 0)$ is proportional to the difference of the $\pi^- p$ and $\pi^+ p$ cross section (cf. Eq. (13)) and, therefore, an empirically accessible quantity. For $-t \approx 0.2$ GeV^2, the helicity non-flip amplitude of the Barger-Phillips fit vanishes by construction and is here in line with the results of the KH80 analysis. The Regge-cut model employs an exponential vertex function and obtains an imaginary amplitude different from the other analyses. For $-t \geq 0.8$ GeV^2, the situation changes: here the Barger-Phillips prediction for $\mathrm{Im}\, M^{++}$ is larger than the KH80 analysis for all energies, whereas the result of our Regge-cut model approaches zero as suggested by the Karlsruhe Helsinki analysis. Suprisingly, the real part of M^{++} of the KH80 analysis exhibits a significant energy dependence for fairly large values of $|t|$ which is neither reproduced by our Regge-cut model nor by the Barger-Phillips parameterization.

5 Conclusions

The experimental search for baryon resonances with masses above 2 GeV requires theoretical analyses based on coupled reaction channel approaches. Partial wave amplitudes provide a convenient summary of the experimental data, but may suffer from convergence problems at large energies. In the high energy limit, two-hadron reactions are diffractive and can be described economically and quantitatively within Regge phenomenology. The corresponding amplitudes offer the possibility to obtain constraints for theoretical approaches from the high energy region. Thus, in lieu of partial waves, amplitudes for forward scattering as predicted by Reggy models may provide an interface between theory and data.

In this paper, we presented a Regge-cut model which reproduces the differential cross sections down to energies $\sqrt{s} \approx 3$ GeV and for momentum transfer $-t < 2$ GeV^2.

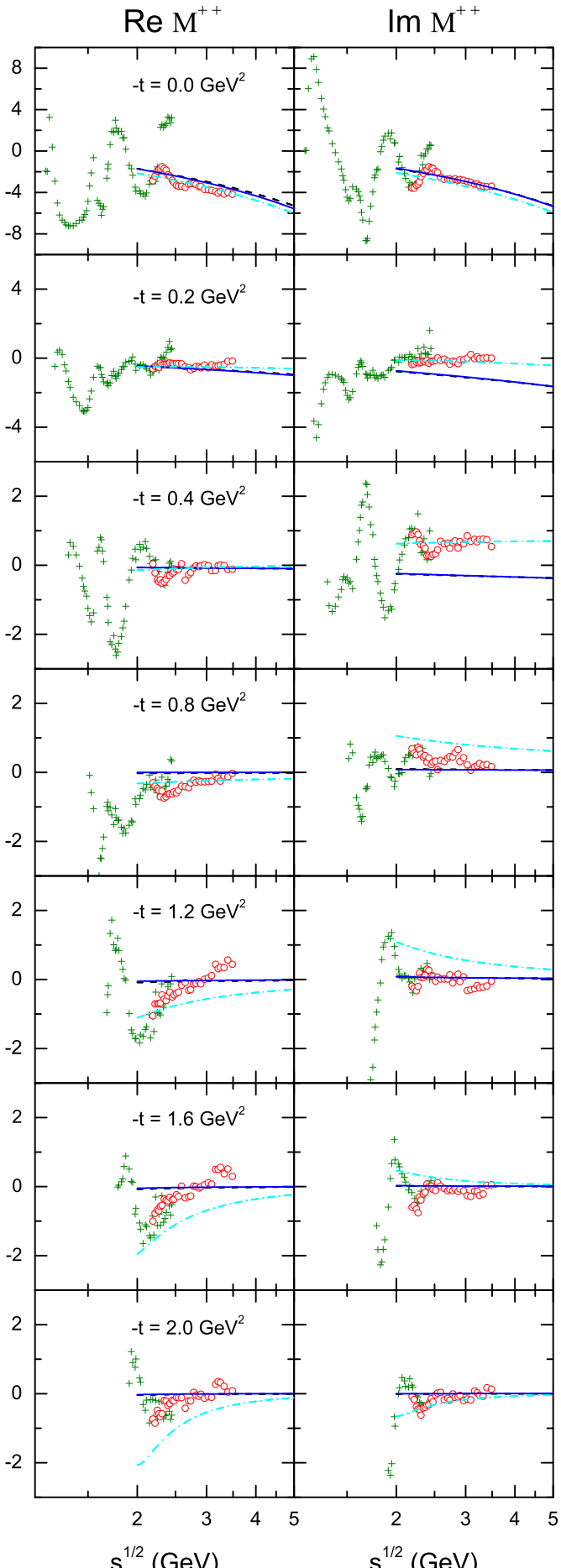

We then compared the resulting amplitudes with those determined in the Karlsruhe-Helsinki (KH80) partial wave analysis. It turned out that the magnitudes of the helicity non-flip amplitudes are not well constrained. There is strong evidence for a rapid decrease with increasing momentum transfer. The amplitudes of the Barger-Phillips fit [31], which we considered here as example of an alternative Regge parameterization, may be taken as an estimate for the upper limit of the helicity non-flip amplitude. The magnitudes of the helicity flip amplitudes derived from the Regge-cut model join the corresponding quantities obtained in the KH80 partial wave analysis smoothly in the vicinity of $\sqrt{s} = 3$ GeV. We conclude that the appropriate energy region for matching meson-nucleon dynamics to diffractive scattering could be around approximately 3 GeV for the helicity flip amplitude of the πN charge-exchange reaction.

This work is partially supported by the Helmholtz Association through funds provided to the virtual institute "Spin and strong QCD" (VH-VI-231), by the EU Integrated Infrastructure Initiative Hadron Physics Project under contract number RII3-CT-2004-506078 and by DFG (SFB/TR 16, "Subnuclear Structure of Matter"). F. H. is grateful for the support from the Alexander von Humboldt Foundation. A.S. acknowledges support by the JLab grant SURA-06-C0452 and the COSY FFE grant No. 41760632 (COSY-085).

References

1. A. V. Sarantsev *et al.*, Phys. Lett. B **659**, 94 (2008) [arXiv:0707.3591 [hep-ph]].
2. I. G. Aznauryan *et al.* [CLAS Collaboration], arXiv:0804.0447 [nucl-ex].
3. R. Nasseripour *et al.* [CLAS Collaboration], Phys. Rev. C **77**, 065208 (2008) [arXiv:0801.4711 [nucl-ex]].
4. M. Sumihama *et al.*, Phys. Lett. B **657**, 32 (2007) [arXiv:0708.1600 [nucl-ex]].
5. C. Amsler *et al.*, Phys. Lett. B **667**, 1 (2008).
6. R. Koch and E. Pietarinen, Nucl. Phys. A **336**, 331 (1980).
7. G. Höhler, Landolt-Börnstein Series, Group I, Elementary Particles, Nuclei and Atoms **9b1**, Springer, Berlin, 1983.
8. R. E. Cutkosky, C. P. Forsyth, R. E. Hendrick and R. L. Kelly, Phys. Rev. D **20**, 2839 (1979).
9. R. A. Arndt, W. J. Briscoe, I. I. Strakovsky, R. L. Workman and M. M. Pavan, Phys. Rev. C **69**, 035213 (2004) [arXiv:nucl-th/0311089].
10. R.A. Arndt, W.J. Briscoe, I.I. Strakovsky and R.L. Workman, Phys. Rev. C **74**, 045205 (2006).
11. R.A. Arndt, W.J. Briscoe, R.L. Workman and I.I. Strakovsky, CNS Data Analysis Center, *http://gwdac.phys.gwu.edu/*
12. I.G. Alekseev *et al.*, Eur. Phys. J. A **12**, 117 (2001).
13. I. G. Alekseev *et al.*, AIP Conf. Proc. **915**, 665 (2007); arXiv:0810.1143 [hep-ex].
14. See the comments of G. Höhler and R.L. Workman in W.M. Yao *et al.*, J. Phys. G **33**, 1 (2006).
15. D. M. Manley and E. M. Saleski, Phys. Rev. D **45**, 4002 (1992).
16. M. Batinić, I. Šlaus, A. Švarc and B. M. K. Nefkens, Phys. Rev. C **51**, 2310 (1995) [Erratum-ibid. C **57**, 1004 (1998)] [arXiv:nucl-th/9501011].
17. M. Batinić, I. Dadić, I. Šlaus, A. Švarc, B. M. K. Nefkens and T. S. H. Lee, Phys. Scripta **58**, 15 (1998).
18. T. P. Vrana, S. A. Dytman and T. S. H. Lee, Phys. Rept. **328**, 181 (2000) [arXiv:nucl-th/9910012].
19. G. Penner and U. Mosel, Phys. Rev. C **66**, 055211 (2002) [arXiv:nucl-th/0207066].
20. N. Kaiser, T. Waas and W. Weise, Nucl. Phys. A **612**, 297 (1997).
21. U.-G. Meißner and J. A. Oller, Nucl. Phys. A **673**, 311 (2000).
22. E. Oset *et al.*, Prog. Part. Nucl. Phys. **61**, 260 (2008) [arXiv:0711.2967 [nucl-th]].
23. E. E. Kolomeitsev and M. F. M. Lutz, Phys. Lett. B **585**, 243 (2004) [arXiv:nucl-th/0305101].
24. O. Krehl, C. Hanhart, S. Krewald and J. Speth, Phys. Rev. C **62**, 025207 (2000) [arXiv:nucl-th/9911080].
25. A. M. Gasparyan, J. Haidenbauer, C. Hanhart and J. Speth, Phys. Rev. C **68**, 045207 (2003) [arXiv:nucl-th/0307072].
26. G. Y. Chen, S. S. Kamalov, S. N. Yang, D. Drechsel and L. Tiator, Phys. Rev. C **76**, 035206 (2007) [arXiv:nucl-th/0703096].
27. B. Julia-Diaz, T. S. Lee, A. Matsuyama and T. Sato, Phys. Rev. C **76**, 065201 (2007) [arXiv:0704.1615 [nucl-th]].
28. B. Julia-Diaz, T. S. Lee, A. Matsuyama, T. Sato and L. C. Smith, Phys. Rev. C **77**, 045205 (2008) [arXiv:0712.2283 [nucl-th]].
29. A. Donnachie and P. V. Landshoff, Phys. Lett. B **296**, 227 (1992) [arXiv:hep-ph/9209205].
30. A. C. Irving and R. P. Worden, Phys. Rept. **34**, 117 (1977).
31. V. Barger and R.J.N. Phillips, Phys. Lett. B **53**, 195 (1974).
32. J. L. Basdevant, C. D. Froggatt and J. L. Petersen, Nucl. Phys. B **72** (1974) 413.
33. B. Ananthanarayan, G. Colangelo, J. Gasser and H. Leutwyler, Phys. Rept. **353** (2001) 207 [arXiv:hep-ph/0005297].
34. S. Descotes-Genon, N. H. Fuchs, L. Girlanda and J. Stern, Eur. Phys. J. C **24** (2002) 469 [arXiv:hep-ph/0112088].
35. J. R. Pelaez and F. J. Yndurain, Phys. Rev. D **71**, 074016 (2005) [arXiv:hep-ph/0411334].
36. J. R. Pelaez and F. J. Yndurain, Phys. Rev. D **69**, 114001 (2004).
37. A. Sibirtsev *et al.*, in preparation.
38. K. G. Boreskov, A. M. Lapidus, S. T. Sukhorukov and K. A. Ter-Martirosyan, Nucl. Phys. B **40**, 307 (1972).
39. W.D. Apel *et al.*, Phys. Lett. B **72**, 132 (1977).
40. V.D. Apokin *et al.*, Z. Phys. C **15**, 293 (1982).
41. A.V. Barnes *et al.*, Phys. Rev. Lett. **37**, 76 (1976).
42. V.N. Bolotov *et al.*, Nucl. Phys. B **73**, 365 (1974).
43. O. Guisan, P. Bonamy, P.Le Du and L. Paul, Nucl. Phys. B **32**, 681 (1971).
44. P. Sonderegger *et al.*, Phys. Lett. **20**, 75 (1966).
45. M.A. Wahlig and I. Mannelli, Phys. Rev. **168**, 1515 (1968).
46. M. Minowa *et al.*, Nucl. Phys. B **294**, 979 (1987).
47. D. Hill *et al.*, Phys. Rev. Lett. **30**, 239 (1973).
48. D.D. Drobnis *et al.*, Phys. Rev. Lett. **20**, 274 (1968).
49. G. Giacomelli, Landolt-Börnstein Series, Group I, Elementary Particles, Nuclei and Atoms **7**, Springer, Berlin, 1973.
50. H.R. Crouch *et al.*, Phys. Rev. D **21**, 3023 (1980).

51. R.M. Brown *et al.*, Nucl. Phys. B **117**, 12 (1976).
52. Y. Suzuki *et al.*, Nucl. Phys. B **294**, 961 (1987).
53. W.S. Brockett *et al.*, Phys. Rev. Lett. **26**, 527 (1971).
54. W.S. Brockett *et al.*, Phys. Lett. B **51**, 390 (1974).
55. A.V. Stirling *et al.*, Phys. Rev. Lett. **14**, 763 (1965).
56. M.E. Sadler *et al.*, Phys. Rev. C **69**, 055206 (2004).
57. Hades Collaboration, *http://www-hades.gsi.de/*
58. A.S. Carroll *et al.*, Phys. Rev. Lett. **33**, 928 (1974).
59. A.S. Carroll *et al.*, Phys. Lett. B **61**, 303 (1976).
60. A. Citron *et al.*, Phys. Rev. **144**, 1101 (1966).
61. S.V. Denisov *et al.*, Nucl. Phys. B **65**, 1 (1973).
62. K.J. Foley *et al.*, Phys. Rev. Lett. **19**, 857 (1967).
63. I. Mannelli, A. Bigi, R. Carrara, M. Wahlig and L. Sodickson, Phys. Rev. Lett. **14**, 408 (1965).
64. M. Fukugita and K. Igi, Phys. Rept. **31**, 237 (1977).
65. W. Melnitchouk, R. Ent and C. Keppel, Phys. Rept. **406**, 127 (2005) [arXiv:hep-ph/0501217].
66. F. Halzen and C. Michael, Phys. Lett. B **36**, 367 (1971).
67. R.L. Kelly, Phys. Lett. B **39**, 635 (1972).
68. P. Johnson, K.E. Lassila, P. Koehler, R. Miller and A. Yokosawa, Phys. Rev. Lett. **30**, 242 (1973).
69. E. Leader and B. Nicolescu, Phys. Rev. D **7**, 836 (1973).
70. K. Goulianos, Phys. Rept. **101**, 169 (1983).